Proc. Natl. Acad. Sci. USA
Vol. 88, pp. 10109–10113, November 1991
Biochemistry

A regulated RNA binding protein also possesses aconitase activity

(iron/ferritin/translational regulation/iron-responsive element/iron-responsive element binding protein)

STAMATINA KAPTAIN, WILLIAM E. DOWNEY, CAREEN TANG, CAROLINE PHILPOTT, DAVID HAILE, DAVID G. ORLOFF, JOE B. HARFORD, TRACEY A. ROUAULT, AND RICHARD D. KLAUSNER*

Cell Biology and Metabolism Branch, National Institute of Child Health and Human Development, National Institutes of Health, Bethesda, MD 20892

Communicated by David R. Davies, August 19, 1991 (received for review July 8, 1991)

ABSTRACT **A clone for the iron-responsive element (IRE)-binding protein (IRE-BP) has been transfected and expressed in mouse fibroblasts. The IRE-BP gene product binds IREs with high affinity and specificity. Amino acid alignments reveal that the IRE-BP is 30% identical to mitochondrial aconitase. The 18 active site residues of mitochondrial aconitase are identical to those in the IRE-BP, suggesting that the IRE-BP may possess aconitase activity. After purification of native IRE-BP and immunoaffinity purification of transfected and expressed IRE-BP, we demonstrate that the purified IRE-BP has aconitase activity.**

Cells of higher eukaryotes regulate the expression of at least two proteins, the transferrin receptor (TfR) and ferritin (Ft), in response to changes in iron availability. The rate of synthesis of the TfR is determined by iron-dependent control of the half-life of the TfR mRNA, whereas Ft synthesis is determined by alterations in the rate of translation initiation (1). It is now clear that a common set of regulatory components underlies both of these phenomena. Both mRNAs contain specific stem–loop structures called iron-responsive elements (IREs) (2), which represent the binding sites for a specific cytoplasmic protein, the IRE-binding protein (IRE-BP) (3, 4). The affinity of the IRE-BP for an IRE changes in response to alterations in the iron status of the cell and is high (10–50 pM) when iron is limiting (5). The iron-responsive switch of RNA-binding affinity involves an as yet undefined posttranslational alteration.

Some of us recently reported the molecular cloning of the human IRE-BP cDNA (6). Sequence analysis demonstrated a striking conservation between the human IRE-BP and mitochondrial aconitase from *Saccharomyces cerevisiae*, pig heart, or beef heart (7). Several features revealed by the sequence comparison had specific implications for the function of the IRE-BP. The x-ray structure of porcine heart mitochondrial aconitase has been solved and demonstrates a four-domain structure that enfolds an active-site cleft (8, 9). Eighteen residues derived from all four domains are positioned in this cleft and are identical in both the pig heart and the yeast mitochondrial aconitases. All of these 18 active-site residues are identical to corresponding residues in sequence alignments to the human IRE-BP, though overall sequence identity between mitochondrial aconitase and the IRE-BP is only approximately 30% (7). Aconitase contains a 4Fe–4S cluster that has the relatively unusual property (shared with a few ferredoxins) of undergoing a reversible conversion to 3Fe–4S *in vitro* (10, 11). The identical placement within the IRE-BP of the cysteines that ligate the metal complex of aconitase suggests that the former is also likely to be an Fe–S complex protein. Moreover, the lability of the fourth iron in purified aconitase provides a working hypothesis for an iron-sensing mechanism of the IRE-BP (7).

MATERIALS AND METHODS

Generation of *in Vitro* Transcripts. Transcripts of radiolabeled ferritin probe were manufactured and used in gel-retardation assays and UV crosslinking studies as previously described (12).

Reconstruction of IRE-BP cDNA Clone. The *Cla* I–*Sac* I 2.6-kilobase (kb) fragment was excised from the multiple cloning site (*Cla* I), and the 3′ end of the open reading frame (*Sac* I) of 8.1 pBluescript (6) and subcloned into pGEM 7Zf(+) (Promega). An oligonucleotide (Applied Biosystems 381A DNA synthesizer) encoding the rest of the open reading frame of the clone (18 amino acids) was subcloned 3′ of the *Sac* I site. The mouse clone was isolated from an amplified λ phage cDNA library (Clontech) after screening with human IRE-BP sequences derived from the 5′ end of 8.1 pBluescript (unpublished observations). The 5′ end of the mouse cDNA was amplified from the λ phage clone by the polymerase chain reaction (PCR) (Perkin–Elmer/Cetus thermal cycler) using 5′ PCR primer sequences corresponding to 12 amino acids of the mouse 5′ end and containing 24 bases upstream from the putative methionine start site. The 3′ PCR primer corresponded to 16 amino acids surrounding the *Pst* I recognition site at position 217 of the previously reported cDNA (6). After amplification, the DNA was cut with *Sph* I (multiple cloning site) and *Pst* I (6) and was subcloned into the 5′ end of the human cDNA. A point deletion at position 2099 in the original clone (6) was corrected by PCR. This mouse/human chimera was subcloned into the *Xba* I site of the expression vector pCDLSRα (13) after several modifications of the vector (an *Xho* fragment was deleted and replaced by a multiple cloning site). Complementary oligonucleotides encoding an endoproteinase recognition sequence (14) followed by an epitope of the Myc protein recognized by the monoclonal antibody 9E10 (15) were inserted between the open reading frame of the IRE-BP cDNA and the Myc epitope cDNA and subcloned into the 3′ end of the chimera using *Bal* I (6) and *Bam*HI (vector).

Transient Transfection Assays. Transient transfection assays were performed as previously described with 20 μg of IRE-BP/Myc cDNA per 100-mm tissue culture dish of mouse B6 cells (16).

Preparation of Lysates and Immunoprecipitation of Transfected IRE-BP/Myc cDNA. Immunoprecipitations were performed as follows. Nontransfected or transfected cells were lysed in lysis buffer containing 1% Triton, 300 mM NaCl, 20 mM Tris·HCl (pH 7.4), and the protease inhibitors leupeptin (Sigma) and *p*-nitrophenyl guanidinobenzoate (Sigma). Human liver lysates were prepared as described (12). After 30 min on ice, insoluble material was pelleted with a 10-min 13,000-rpm spin in a Beckman Microfuge. Anti-Myc antibody (8 μl of mouse ascites) was preadsorbed to protein G-Sepharose beads, and cell lysate was tumbled with anti-Myc-

The publication costs of this article were defrayed in part by page charge payment. This article must therefore be hereby marked "*advertisement*" in accordance with 18 U.S.C. §1734 solely to indicate this fact.

Abbreviations: IRE, iron-responsive element; IRE-BP, IRE-binding protein; TfR, transferrin receptor; Ft, ferritin; H chain, heavy chain.

*To whom reprint requests should be addressed.

```
Protein  sequence    889 a.a.   MKNPFAHLAEPL ... GILNYMIRKMAK

         |   10      |   20      |   30      |   40      |   50      |   60
   1 MKNPFAHLAE PLDAAQPGKR FFNLNKLEDS  RYGRLPFSIR VLLEAAVRNC DEFLVKKNDI 60
  61 ENILNWNVMQ HKNIEVPFKP ARVILQDFTG  VPAVVDFAAM RDAVKKLGGD PEKINPVCPA 120
 121 DLVIDHSIQV DFNRRADSLQ KNQDLEFERN  RERFEFLKWG SQAFHNMRII PPGSGIIHQV 180
 181 NLEYLARVVF DQDGYYYPDS LVGTDSHTTM  IDGLGILGWG VGGIEAEAVM LGQPISMVLP 240
 241 QVIGYRLMGK PHPLVTSTDI VLTITKHLRQ  VGVVGKFVEF FGPGVAQLSI ADRATIANMC 300
 301 PEYGATAAFF PVDEVSITYL VQTGRDEEKL  KYIKKYLQAV GMFRDFNDPS QDPDFTQVVE 360
 361 LDLKTVVPCC SGPKRPQDKV AVSDMKKDFE  SCLGAKQGFK GFQVAPEHHN DHKTFIYDNT 420
 421 EFTLAHGSVV IAAITSCTNT SNPSVMLGAG  LLAKKAVDAG LNVMPYIKTS LSPGSGVVTY 480
 481 YLQESGVMPY LSQLGFDVVG YGCMTCIGNS  GPLPEPVVEA ITQGDLVAVG VLSGNRNFEG 540
 541 RVHPNTRANY LASPPLVIAY AIAGTIRIDF  EKEPLGVNAK GQQVFLKDIW PTRDEIQAVE 600
 601 RQYVIPGMFK EVYQKIETVN ESWNALATPS  DKLFFWNSKS TYIKSPPFFE NLTLDLQPPK 660
 661 SIVDAYVLLN LGDSVTTDHI SPAGNIARNS  PAARYLTNRG LTPREFNSYG SRRGNDAVMA 720
 721 RGTFANIRLL NRFLNKQAPQ TIHLPSGEIL  DVFDAAERYQ QAGLPLIVLA GKEYGAGSSR 780
 781 DWAAKGPFLL GIKAVLAESY ERIHRSNLVG  MGVIPLEYLP GENADALGLT GQERYTIIIP 840
 841 ENLKPQMKVQ VKLDTGKTFQ AVMRFDTDVE  LTYFLNGGIL NYMIRKMAK            889
         |   10      |   20      |   30      |   40      |   50      |   60
```

FIG. 1. Amino acid sequence of the full coding region of the chimeric IRE-BP cDNA. Residues 1–85 are deduced from a mouse cDNA, and the remaining 804 residues are deduced from the human cDNA.

coated beads for 1 hr. Equal amounts of A2B4 ascites (17) were preadsorbed to protein G-Sepharose in similar fashion for use as the irrelevant antibody control. After five washes (1 ml each) with lysis buffer, material was either eluted from the beads with sample buffer (18) or assayed while attached to the beads per the aconitase assay described below. Eluted material was analyzed by SDS/PAGE (18) and silver staining (Bio-Rad). Metabolic labeling with [^{35}S]methionine (Amersham) was performed as described (16) and 1×10^9 cpm of radiolabeled lysate was immunoprecipitated.

Affinity Purification of IRE-BP Derived from Liver. Affinity purification on an IRE affinity column was performed as described (12).

Activation of IRE-BP. Activation of aconitase enzyme for the immunoaffinity-purified IRE-BP activity was performed as follows. Protein G-Sepharose beads (Pharmacia) to which anti-Myc antibody was bound were tumbled for 1 hr with lysates prepared in lysis buffer as described above. Beads were washed five times with phosphate-buffered saline and subsequently centrifuged for 10 min in a Speed Vac (Savant). Samples were then tumbled in anaerobically prepared solutions of 100 mM Tris·HCl (pH 7.4) to which 100 μM sodium citrate, 50 mM dithiothreitol, and 40 μM $Fe(NH_4)_2(SO_4)_2$ was added. Manipulations were performed in an anaerobic glovebag (Instruments for Research and Industry, Cheltenham, PA). Some samples were treated with EGTA (1 mM final concentration) immediately after addition of dithiothreitol and prior to addition of ferrous ammonium sulfate. "Unactivated" samples were tumbled for 10 min at room temperature in the same Tris/citrate buffer with neither dithiothreitol nor Fe^{2+}.

Aconitase Assays. The aconitase assay was performed as follows. After activation, the beads were washed five times in 1 ml of 100 mM Tris·HCl (pH 7.4)/0.1% Triton/100 μM sodium citrate and then divided into aliquots. To each tube was added the aconitase detection mix consisting of 150 mM Tris·HCl, 8.6 mM *cis*-aconitic acid (Sigma) adjusted to pH 8.0, 60 mM $MgCl_2$, 0.04 unit of isocitrate dehydrogenase (Boehringer Mannheim) per ml, 125 μM NADP (Boehringer Mannheim), 240 μM MTT (3-[4,5-dimethylthiazol-2-y]-2,5-diphenyl tetrazolium bromide) (Sigma), and 80 μM phenazine methosulfate (Sigma). Tubes were then tumbled for the time indicated, the beads were pelleted, and A_{560} of the supernatant was measured. Background was determined by excluding *cis*-aconitic acid from the reaction mix. The A_{560} value of a tumbled equivalent sample lacking only the *cis*-aconitic acid substrate was then subtracted from that of its partner to yield the aconitase-specific activity recorded above.

Gel-Retardation Assays with the Porcine Aconitase IRE. A sequence that conforms to a consensus IRE (19) is present in the 5′ untranslated region of the porcine aconitase clone (20). The sequence in the mRNA is 5′-UCAUCUUUGUCAGUGCACAAAAUGG-3′. Radiolabeled RNA corresponding to

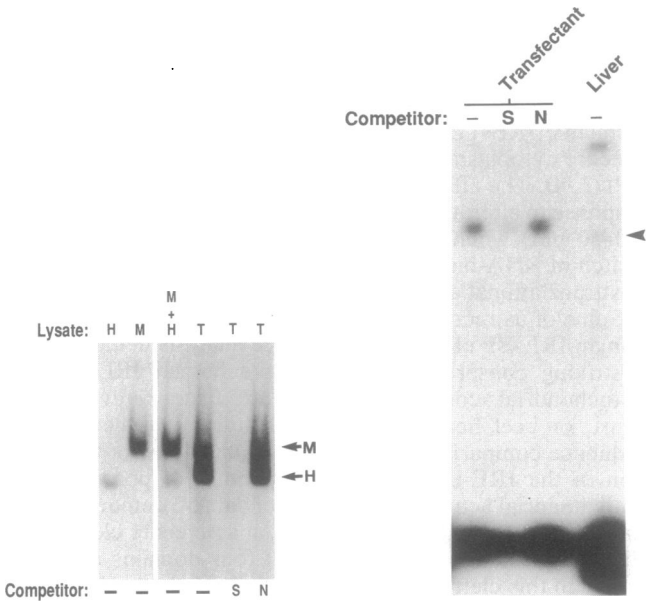

FIG. 2. (*Left*) Expression of the chimeric human IRE-BP after cloning into an expression vector and transfection into mouse B6 fibroblasts. Lysates and gel retardation assays shown are from untransfected mouse B6 lysates (lane M), human liver lysates (lane H), mouse and human lysates mixed *in vitro* (lane M+H), and mouse B6 lysates transfected with either the non-Myc tagged IRE-BP (lanes TT), or vector alone (not shown). Molar excesses (100-fold) of specific competitor (S) or tRNA as a nonspecific competitor (N) demonstrate the specificity of the RNA–protein complex. (*Right*) uv crosslinking of [^{32}P]CTP-labeled IRE RNA to unlabeled mouse lysates prepared from cells transfected with human IRE-BP. The arrowhead denotes the position of a band representing cross-linking of native protein from pig liver lysate in the lane labeled liver. Specifically cross-linked IRE-BP/Myc after immunoprecipitation is located at a slightly higher position in the gel. A 100-fold molar excess of specific (S) unlabeled IRE eliminates the visible complex, whereas a 100-fold molar excess of nonspecific tRNA (N) does not eliminate the complex.

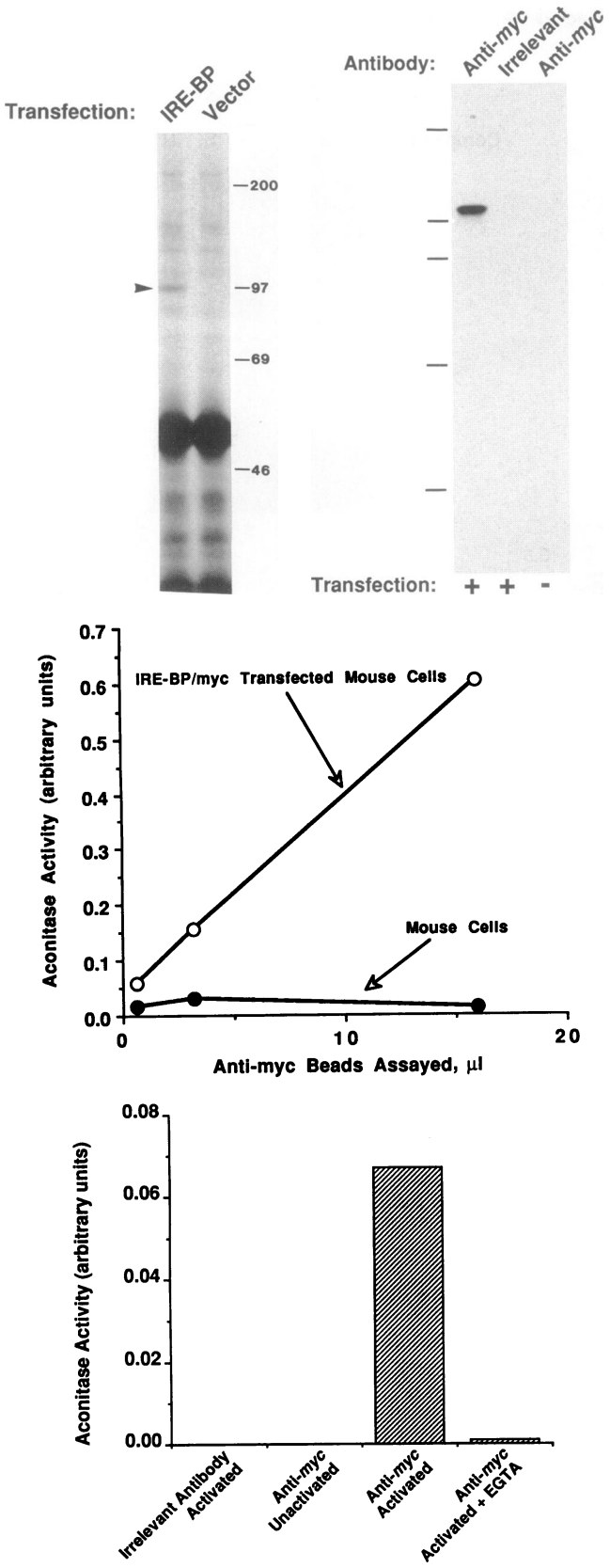

FIG. 3. (*Top Left*) Silver staining (Bio-Rad) of eluates of IRE-BP/Myc transfectants analyzed by SDS/PAGE after immunoprecipitation of lysates from cells transfected with IRE-BP/Myc or with vector alone. IRE-BP/Myc transfectants were also immunoprecipitated with an irrelevant antibody (data not shown). The arrow denotes the specifically immunoprecipitated protein. (*Top Right*) Immunoaffinity purification of IRE-BP/Myc. After a 1-hr metabolic labeling with [^{35}S]methionine, B6 fibroblasts transfected with IRE-BP/Myc were immunoprecipitated with anti-Myc antibody or with an irrelevant antibody and were compared with anti-Myc immunoprecipitation of B6 cells transfected with vector alone. (*Middle*) Aconitase activity of IRE-BP/Myc. Indicated amounts of anti-Myc resin with bound IRE-BP/Myc derived from a transfection of IRE-BP/Myc were activated and then assayed for 3 hr. (*Bottom*) Aconitase activity of IRE-BP/Myc requires activation that is blocked by EGTA. Lysates from cells transfected with IRE-BP/Myc were immunoprecipitated with an irrelevant monoclonal antibody, and with equal amounts of anti-Myc resin that was immunoprecipitated without activation or activated after immunoprecipitation by addition of dithiothreitol and ferrous ammonium sulfate or activated in the presence of 1 mM EGTA. Absorbance at 560 nm was evaluated after 2 hr.

this sequence was transcribed as described (5) and used in gel retardation assays.

RESULTS AND DISCUSSION

In our initial cloning of the IRE-BP cDNA, we isolated what appeared to be a truncated or faulty cDNA because the predicted protein product was 88 kDa, whereas the IRE-BP had a somewhat larger observed mass by SDS/PAGE. In addition, the cDNA could not be expressed as a functional protein as assessed by binding to an IRE-containing RNA. After some difficulty in extending the 5′ end of the human clone, we isolated a murine cDNA containing the 5′ portion of the cDNA. The murine and human cDNA clones were 95% identical over a shared region corresponding to 350 amino acids, and in the murine clone an additional 72 amino-terminal residues were present, resulting in a predicted molecular mass of the total protein of 98.33 kDa (Fig. 1). A hybrid cDNA was constructed that contained nucleotides encoding 85 amino-terminal amino acids derived from the murine IRE-BP and 804 amino acids derived from the human cDNA, and this hybrid construct was cloned into a modified pCDLSRα expression vector and transfected into murine B6 fibroblasts. An RNA gel retardation assay was performed to assess whether the expressed chimeric clone possessed IRE-binding activity. The human IRE-BP can be distinguished from the murine IRE-BP because they have different mobilities in the gel retardation assay (21). The expressed IRE-BP yields a band with a mobility that closely approximates that of the human IRE-BP–IRE complex and is readily distinguishable from the endogenous mouse complex by using an RNA probe corresponding to the human ferritin H chain IRE (Fig. 2 *Left*). The RNA binding activity of the expressed protein showed the same specificity as the endogenous IRE-BP. A complete binding curve allowed us to calculate an affinity of 70 pM for the interaction between the expressed protein and the Ft IRE (not shown), demonstrating that we had indeed expressed a functional, specific IRE-BP. To allow purification of the expressed cloned IRE-BP, we added a 13-amino acid Myc epitope at the carboxyl terminus. The Myc-tagged protein (IRE-BP/Myc) was shown to be functional by gel-retardation assays where it produced a specific high-affinity complex of slightly altered mobility, when compared with the untagged expressed protein (data not shown). In addition, when a lysate of cells expressing the Myc-tagged protein was incubated with a radioactive IRE-containing RNA and subjected to UV crosslinking, the specifically cross-linked material could be immunoprecipitated with a monoclonal anti-Myc antibody (Fig. 2 *Right*).

The Myc tag permitted rapid immunoaffinity purification of the cloned IRE-BP expressed in murine cells. The purity of the precipitated product was assessed by SDS/PAGE and evaluated by either silver staining (Fig. 3 *Top Left*) or autoradiography of the eluate after metabolic labeling (Fig. 3 *Top Right*). In both cases, a specific band of approximately

98–100 kDa was observed. Immunoaffinity-purified protein was then used to determine whether the purified product of the human IRE-BP clone possessed aconitase activity. It has been known for about 20 years that cells contain, in addition to the mitochondrial aconitase, a cytosolic aconitase encoded by a gene found on human chromosome 9 (22). The cytosolic aconitase has previously eluded large-scale purification to homogeneity, and its role in the cytosol has been the subject of a long-standing debate (22, 23). The recent localization of the human IRE-BP gene to chromosome 9 (6) and the perfect conservation of the predicted active site residues suggested the possibility that the IRE-BP is the cytosolic aconitase. Using a specific colorimetric assay, we were indeed able to demonstrate aconitase activity (Fig. 3 *Middle*). When purified, mitochondrial aconitase readily loses the fourth iron from its cluster and must be "activated" by the addition of iron under reducing and anaerobic conditions (10). We found that the same protocol that successfully activates the mitochondrial enzyme was essential for maximal aconitase activity of the immunoaffinity-purified IRE-BP. In the absence of activation, enzymatic activity was extremely low or undetectable relative to activated material. Addition of EGTA, a chelator of ferrous and ferric iron (24), prevented activation in the presence of the usual amounts of dithiothreitol and ferrous ammonium sulfate (Fig. 3 *Bottom*). Results of a single representative experiment are shown. Variations in transfection efficiency resulted in a wide range of absolute values for aconitase activity that made collation of values difficult. At this point, we do not know the fraction of the expressed IRE-BP that is enzymatically competent, so we cannot meaningfully evaluate the specific activity of the aconitase.

In addition to these studies of the expressed protein, we utilized an RNA affinity chromatography column similar to that used initially to purify the IRE-BP to evaluate whether the endogenous IRE-BP possessed aconitase activity. Pig liver lysate was subjected to affinity chromatography by using a matrix coupled to RNA that contained either a functional IRE or a reverse sequence of the IRE stem–loop that shows no specificity for the IRE-BP. A single round of such a purification resulted in a 10-fold enrichment in IRE-binding activity as judged by band shift (Fig. 4 *Upper*). We have previously shown that the only protein specifically enriched by the IRE-containing matrix is the IRE-BP (12). As predicted by the results with the cloned protein, this IRE matrix produced a specific enrichment in aconitase activity (Fig. 4 *Lower*). Finally, we have observed that a bacterially expressed form of the cloned IRE-BP also has aconitase activity (not shown).

The cloning of the IRE-BP provides us with an essential component with which we can study the molecular details of a highly regulated metabolic system that is based upon mRNA-protein interactions. The recognition that the IRE-BP has enzymatic activity has implications for both the function of the protein and its possible evolution. The conservation in the IRE-BP of all the active site residues of the mitochondrial aconitase is consistent with our demonstration that the IRE-BP is a cytosolic aconitase, and it strengthens the prediction that the IRE-BP is built around the structure of aconitase. Most importantly, it lends strong credence to the prediction that the IRE-BP is an [Fe–S] complex protein. We previously proposed that the 3Fe to 4Fe conversion may be the basis for sensing iron levels (7). Evidence that the IRE-BP senses available intracellular iron (25, 26) would require a reversible binding mechanism such as that suggested for these labile [Fe–S] complexes. The requirement for the "activation" of the purified IRE-BP by loading with Fe utilizing a protocol similar to that which is used to add the fourth iron and activate the mitochondrial aconitase (10) strongly points to the lability of the predicted IRE-BP Fe–S

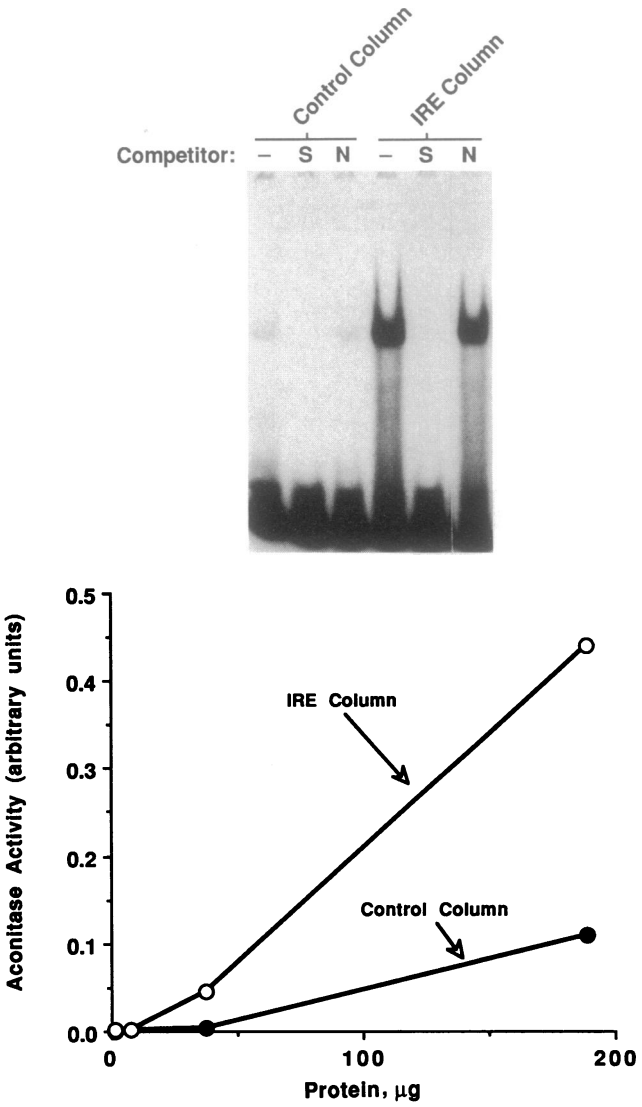

FIG. 4. (*Upper*) Gel retardation assays of eluted proteins derived from affinity purification of pig liver lysates from either a control column or an IRE column. S denotes addition of a 100-fold molar excess of unlabeled IRE (specific; lanes S) and N denotes competition with a 100-fold molar excess with tRNA (nonspecific; lanes N). (*Lower*) Aconitase activity of affinity-purified IRE-BP from pig liver. Dilutions of eluates from control and IRE-affinity columns were activated, and the indicated amounts of protein were assayed after a 30-min reaction.

center. Exactly how the state of the Fe–S center affects RNA binding remains to be demonstrated.

An interesting relationship between the IRE-BP and the mitochondrial enzyme is further suggested by the presence of an IRE in the 5′ untranslated region of the mRNA encoding porcine mitochondrial aconitase. This porcine mitochondrial aconitase (19, 20) IRE binds the IRE-BP with an affinity that closely approximates the binding affinity of the IRE-BP for the ferritin H chain IRE (data not shown). Purified pig heart mitochondrial aconitase does not appear to bind the ferritin H chain IRE as judged by gel retardation studies (data not shown). However, gene duplication of mitochondrial aconitase and subsequent mutation may have resulted in a cytosolic form of aconitase that evolved into the high-affinity cytosolic IRE-BP. The IRE-BP has numerous regions of amino acid insertions relative to mitochondrial aconitase that are likely to reside on the surface of the molecule (7). Some of these surface loops may play a role in RNA binding. Through evolution, the RNA binding protein maintained all

of the predicted active site residues of aconitase; thus, preservation of aconitase enzymatic activity may be essential for some aspect of IRE-BP function. Whether such a scenario has been used in the development of other mRNA binding regulatory proteins may become evident as other posttranscriptional control systems are elucidated.

We thank Howard Zalkin for his generous gift of purified mitochondrial aconitase. We thank Drs. Helmut Beinert, Mary Claire Kennedy, and C. David Stout for stimulating discussions of this material. S.K. acknowledges the support of the Howard Hughes Medical Institute National Institutes of Health Research Scholars Program.

1. Klausner, R. D. & Harford, J. B. (1989) *Science* **246,** 870–872.
2. Hentze, M. W., Caughman, S. W., Rouault, T. A., Barriocanal, J. G., Dancis, A., Harford, J. B. & Klausner, R. D. (1987) *Science* **238,** 1570–1573.
3. Leibold, E. A. & Munro, H. N. (1988) *Proc. Natl. Acad. Sci. USA* **85,** 2171–2175.
4. Rouault, T. A., Hentze, M. W., Caughman, S. W., Harford, J. B. & Klausner, R. D. (1988) *Science* **241,** 1207–1210.
5. Haile, D. J., Hentze, M. W., Rouault, T. A., Harford, J. B. & Klausner, R. D. (1989) *Mol. Cell. Biol.* **9,** 5055–5061.
6. Rouault, T. A., Tang, C. K., Kaptain, S., Burgess, W. H., Haile, D. J., Samaniego, F., McBride, O. W., Harford, J. B. & Klausner, R. D. (1990) *Proc. Natl. Acad. Sci. USA* **87,** 7958–7962.
7. Rouault, T. A., Stout, C. D., Kaptain, S., Harford, J. B. & Klausner, R. D. (1991) *Cell* **64,** 881–883.
8. Robbins, A. H. & Stout, C. D. (1989) *Proteins* **5,** 289–312.
9. Robbins, A. H. & Stout, C. D. (1989) *Proc. Natl. Acad. Sci. USA* **86,** 3639–3643.
10. Beinert, H. & Kennedy, M. C. (1989) *Eur. J. Biochem.* **186,** 5–15.
11. George, S. J., Armstrong, F. A., Hatchikian, E. C. & Thomson, A. J. (1989) *Biochem. J.* **264,** 275–284.
12. Rouault, T. A., Hentze, M. W., Haile, D. J., Harford, J. B. & Klausner, R. D. (1989) *Proc. Natl. Acad. Sci. USA* **86,** 5768–5772.
13. Takebe, Y., Seiki, M., Fujisawa, J., Hoy, P., Yokota, K., Arai, K., Yoshida, M. & Arai, N. (1988) *Mol. Cell. Biol.* **8,** 466–472.
14. Schlotissek, S. & Grosse, F. (1988) *Gene* **62,** 55–64.
15. Pelham, H. R. (1988) *EMBO J.* **7,** 913–918.
16. Casey, J. L., Di Jeso, B., Rao, K., Klausner, R. D. & Harford, J. B. (1988) *Proc. Natl. Acad. Sci. USA* **85,** 1787–1791.
17. Samelson, L. E., Germain, R. N. & Schwartz, R. H. (1983) *Proc. Natl. Acad. Sci. USA* **80,** 6972–6976.
18. Laemmli, U. K. (1970) *Nature (London)* **227,** 680–685.
19. Harford, J. B. & Klausner, R. D. (1990) in *Post-Transcriptional Control of Gene Expression*, eds. McCarthy, J. E. G. & Tuite, M. F. (Springer, Berlin), pp. 399–409.
20. Zheng, L., Andrews, P. C., Hermodson, M. A., Dixon, J. E. & Zalkin, H. (1990) *J. Biol. Chem.* **265,** 2814–2821.
21. Hentze, M. W., Seuanez, H. N., O'Brien, S. J., Harford, J. B. & Klausner, R. D. (1989) *Nucleic Acids Res.* **17,** 6103–6108.
22. Shows, T. B. & Brown, J. A. (1977) *Cytogenet. Cell Genet.* **19,** 26–37.
23. Spoto, G. (1984) *IRCS Med. Sci.* **12,** 979–980.
24. Martell, A. E. & Smith, R. M. (1977) in *Critical Stability Constants* (Plenum, New York), Vol. 1, pp. 269–271.
25. Rouault, T., Rao, K., Harford, J., Mattia, E. & Klausner, R. D. (1985) *J. Biol. Chem.* **260,** 14862–14866.
26. Rogers, J. & Munro, H. N. (1987) *Proc. Natl. Acad. Sci. USA* **84,** 2277–2281.